Proceedings of the International Conference on Creationism

Volume 9
Print Reference: 267-279

Article 9

2023

A Rapid Ice Age and Transition to Ice Sheet Growth

Steven M. Gollmer
Cedarville University

Recommended Citation

Gollmer, Steven M. (2023) "A Rapid Ice Age and Transition to Ice Sheet Growth," *Proceedings of the International Conference on Creationism*: Vol. 9, Article 9.
DOI: 10.15385/jpicc.2023.9.1.16
Available at: https://digitalcommons.cedarville.edu/icc_proceedings/vol9/iss1/9

Gollmer, S.M. 2023. A rapid ice age and transition to ice sheet growth. In J.H. Whitmore (editor), *Proceedings of the Ninth International Conference on Creationism*, pp. 267-279. Cedarville, Ohio: Cedarville University International Conference on Creationism.

CEDARVILLE UNIVERSITY

9th ICC 2023

A RAPID ICE AGE AND TRANSITION TO ICE SHEET GROWTH

Steven M. Gollmer, Cedarville University, School of Science and Mathematics, 251 N. Main St., Cedarville, Ohio 45314 USA
gollmers@cedarville.edu

ABSTRACT

For the past half-century, creationists have explored different explanations for glacial erosion features across the Northern Hemisphere. The best explanation to date is a single post-flood ice age with multiple surges. The challenge with this model is the limited time available between the end of the Flood and the time of Abraham, which appears to be post ice age. Oard (1979) proposed a short post-flood ice age developing due to warm oceans, volcanic aerosols, and barren surfaces. Performing computer climate simulations, Spelman (1996), Vardiman (1998), Gollmer (2013), and Gollmer (2018) verified that enhance precipitation occurs at higher latitudes due to a warm Arctic Ocean. However, this precipitation is in the form of rain. In addition, the precipitation primarily falls over oceans rather than land, which is necessary for the buildup of ice sheets.

Using a climate model with a dynamic atmosphere and ocean, this paper reports on a multi-century climate simulation that begins with warm oceans and an enhanced stratospheric aerosol layer. The length of the simulation allows oceans with a uniform temperature of 24 °C to transition towards modern day values. Initial cooling of the oceans results in surface water penetrating to great depths. After sufficient cooling, the surface circulation decouples from the deep ocean due to the development of a thermocline. This transition in ocean circulation may have implications when interpreting proxy climate data.

Once the oceans sufficiently cool, snow can accumulate at higher latitudes and initiate the buildup of ice sheets. Ocean circulation, precipitation patterns, and annual snow accumulation are examined to evaluate the feasibility of an ice age initiated by a warm ocean. The timing of ice sheet initiation also provides a reference point from which to associate other post-flood events. Finally, limitations to this modeling method are discussed and future research opportunities are proposed

KEY WORDS

Climate Modeling, Ice Age

I. INTRODUCTION

When developing a young earth creationist (YEC) model, we carefully use Scripture to provide insights on processes and timing of events. We recognize as Schaeffer (1972) does, that "where it (the Bible) speaks of the cosmos, science, what it says is true. Likewise, where it touches history, it speaks with that I call true truth, that is propositional, objective truth" (p. 76). Unfortunately, Scriptures do not provide a comprehensive narrative of earth history. It is, therefore, up to us to propose scenarios that synthesize what God has revealed about earth history with what we have learned about the lawfulness of God's creation through science.

Objecting to Lyell' statement "the present is the key to the past" (Lyell 1833), scriptural geologists of the nineteenth century looked to the Genesis Flood to explain extensive geological deposits around the globe. Whitcomb and Morris' (1961) *The Genesis Flood: The Biblical Record and Its Scientific Implications* systematized what was known of the Deluge and proposed solutions to objections to flood geology. In the subsequent half-century, progress was made across multiple fronts; including radiometric dating (Vardiman et al. 2005), plate tectonics (Austin et al. 1994), and sedimentology (Whitmore and Garner 2018). In each of these cases, rates of current processes are not a key to the past. This also applies to interpreting glacial features generated in the wake of the Flood.

Although alternate explanations for extensive glacial features in North America, Europe, and Asia are provided by Cox (1979), Molén (1990), and Oard (1997), most YECs agree with Whitcomb and Morris that a post-flood ice age provides the best explanation. Unlike secular models, that used to posit four ice advances in North America over the course of a million years (Luthi et al, 2008), Oard (1979) proposes a single ice age of duration 500 years. In this scenario, the post-flood ocean is warm due to heat released by the rapid tectonic motion of continents, volcanism, and turbulent mixing. The post-flood world underwent significant mountain building and volcanic activity. This results in stratospheric aerosols, which have a cooling effect on the atmosphere. Oard (1990) elaborates on his scenario and provides the details needed to test it using climate models.

Using the National Center for Atmospheric Research (NCAR) Community Climate Model 1 (CCM1), Spelman (1996) tested the sensitivity of the atmosphere to warm post-flood oceans. Setting sea surface temperatures to 30 °C, regardless of latitude, resulted in enhanced arctic precipitation commensurate with what is needed to generate a 400 m thick ice sheet within 500 years. Vardiman (1998) used the same model to test the impact of ocean hot spots over the Mid-Atlantic ridge. This resulted in shifted wind patterns and enhanced downwind precipitation.

Gollmer (2013) verified Spelman's warm sea surface temperature scenario using the Goddard Institute of Space Studies (GISS) ModelE. Unlike CCM1, ModelE has a dynamic ocean coupled to the atmosphere. This allows the ocean temperature to develop over time. With an initial ocean temperature of 30 °C, both at depth and high latitudes, the tropical oceans become unreasonably hot several years into the simulation. Stratospheric aerosols with an optical thickness of 2.0 were added to mitigate heat coming from the warm ocean surface. Even with aerosols, this initial ocean temperature is too high.

An additional problem with these simulations is the form and location of precipitation. The elevated temperature of the ocean has a corresponding effect on the atmosphere, resulting in precipitation in the form of rain rather than snow. High precipitation events in the Arctic occur over the ocean, not land. With warm oceans, high pressure systems develop over the cooler land. This results in thermal winds that flow to low pressure systems over the ocean.

Doubling the GISS ModelE's resolution, Gollmer (2018) explored the impact of aerosol distribution on precipitation patterns for the post-flood ice age scenario. Ocean temperatures were initialized at a lower temperature of 24 °C, which is in line with arctic ocean temperatures inferred from marine sediment cores by Sluijs et al. (2006). Although non-uniform aerosol distributions shift the jet stream, and in turn precipitation patterns, it was not enough to provide enhanced precipitation over land at high latitudes. Even with the reduction of initial ocean temperature, during the six-year sensitivity study there was insufficient cooling to allow snowfall or ice accumulation needed for initiating an ice age.

Given these results, episodic high precipitation events are seen as a possible source of snowfall needed to initiate an ice age. Vardiman (2003) explored the impact of hypercanes forming over warm oceans using a mesoscale model. These models divide the earth's surface into cells 30 km on a side or smaller. Operating with cells twenty times larger in length and width, global circulation models fail to capture sub-scale processes, which can generate significant precipitation events. Vardiman and Brewer (2010, 2011, and 2012) used the NCAR Weather Research and Forecasting Model (WRF) to simulate the impact of warm oceans on Yellowstone, the Middle East, and the Eastern United States respectively.

Although mesoscale simulations may provide answers to high precipitation events over land, they do not provide a description of what is happening at the global scale. As already seen, warm ocean simulations result in precipitation in the form of rain everywhere except at high altitudes. This necessitates global simulations that extend beyond sensitivity studies.

The purpose of this study is to provide a multi-century simulation at the global scale. This provides time for oceans with uniform temperatures to cool and establish circulation patterns due to temperature differences. In turn, the atmosphere cools to the point where snow can accumulate. The next section of this paper describes the climate model used and its boundary and initial conditions. The following section presents the results and commentary of how different oceanic and atmospheric values change over time. This paper concludes with a discussion of relevant observations and proposed future research.

II. FOUR CENTURY CLIMATE MODEL RUN

Since the 1950s, numerous global circulation models (GCMs) have been developed. A model's success is gauged by how accurately it predicts long-term temperature, precipitation, and wind patterns for the present climate. In the past seventy years, these models have incorporated sophisticated ocean/atmosphere, land/vegetation, and dynamic sea/land ice interactions. The complexity of these models can no longer be maintained and advanced by a single researcher. Therefore, communities of researchers formed to focus their efforts in developing the best climate models.

The Third Coupled Model Intercomparison Project (CMIP3) was released in 2007 in conjunction with the Fourth Assessment Report (AR4) of the Intergovernmental Panel on Climate Change (IPCC). It consisted of twenty-five models from eighteen research groups (PCMDI, 2007). Poorly understood feedbacks involving the carbon cycle and clouds were the focus of CMIP5. By 2013 GCMs were incorporating new parameterizations to provide better results related to these physical processes. CMIP5 involved forty GCMs from twenty research groups (Kamworapan and Surussavadee 2019). This in turn provided projections of climate change used by IPCC AR5. CMIP6 continues to incorporate more accurate representations of biogeochemical processes. To date, there are one hundred models from forty-nine modelling groups contributing to this effort (Hausfather 2019). Results from these models are used in AR6, which is still in development.

Recognizing the need to use a vetted GCM, Gollmer (2013) used the Goddard Institute of Space Studies Model E, which was part of AR4. The horizontal resolution of this model was 5° longitude by 4° latitude, with 20 atmospheric layers. It included a coupled-ocean model consisting of the same horizontal resolution and 13 ocean layers. Gollmer (2018) used the AR5 update of the GISS Model E2 (Hansen et al. 1983). This included improvements in calculations of microphysics and other physical effects (Schmidt et al. 2014). At the expense of computational time, the resolution was doubled by representing the atmosphere with cells of 2.5° longitude by 2° latitude and 40 layers. The ocean consisted of 32 layers. Both Gollmer (2013) and (2018) did sensitivity studies, which looked at changes in atmospheric parameters due to changed initial and boundary conditions. These conditions include the following: increased uniform ocean temperature, thick stratospheric aerosols, removal of sea ice, and removal of ice sheets in Greenland and Antarctica.

This paper reports on a simulation using the GISS Model E2.1.2, which incorporates improvements linked to CMIP6 (Kelley et al. 2020). With the need to simulate ocean cooling from an initial uniform temperature of 24 °C, a 400-year model run was performed. Given this extended time, it was necessary to drop the resolution back to 5° longitude by 4° latitude with 20 atmospheric layers and 13 ocean layers. Although the resolution was reduced, model improvements added since AR4 were still enabled. In this configuration, one year of model time was simulated in four hours on a 2.5 GHz Intel i3 using two threads. Model statistics were saved for each month of the run.

This simulation changes the initial and boundary conditions but not the software code. Initial ocean temperature is uniformly set at 24 °C and stratospheric aerosols set at an optical thickness of 2.0. Unlike Gollmer (2018), the aerosol distribution is uniform from North to South Pole. The ice sheets covering Antarctica and Greenland are removed and isostatic adjustments made to land elevation. The exposed ground is not assigned vegetation and, therefore, treated as bare ground for calculating albedo and moisture retention. The final change involved removing sea ice.

Although diligence was given to change initial and boundary conditions, there are some artifacts that slipped through. First year data indicates that some land ice near the coast is still present. Given the length of the model run, this ice quickly disappears due to the temperature of the ocean. Also, when calculating isostatic rebound, some underwater land features become exposed near the coastline. This causes the model to fail due to inconsistent boundary conditions. Since the source of the inconsistency could not be tracked down, rebound was not allowed to cause an ocean grid cell to become land. Given that this problem occurs over a small region, it is assumed this does not change the simulation results significantly.

One final note regarding topography. Current day ocean basins and continent positions are used rather than inferring a different configuration. Assuming post-flood contributions to the geological column include some if not all the Cenozoic, this simulation fails to account for changes in continent position, exposure of land surfaces due to a lowering sea level, and mountain building events. Incorporating these factors into the model would require constant changes in configuration. Any heating of the oceans due to these factors is assumed to occur before the model simulation. For the sake of comparisons with climate proxy data, this model is effectively a simulation occurring during the Quaternary Period with high stratospheric aerosols, warm oceans, and missing land and sea ice.

III. RESULTS

Model E2 reports monthly accumulated statistics on over a thousand data fields. Some are used for diagnostics and others for reporting the state of the model. Since this paper focuses on the feasibility of a rapid post-flood ice age, only temperature and precipitation fields are described and commented on. Progression of the model is evaluated by comparing these data fields at different years within the simulation. Ideally, the simulation will transition from the initial condition of warm oceans to that of the modern day. A reference model is run to provide data fields corresponding to the unmodified model. These fields are referred to as either the reference or modern-day conditions.

A. Ocean basin temperature

Oceans at all depths are initialized at 24 °C. At the end of the first year, sea surface temperature in the Arctic cools to 18 °C while the equator warms to 25 °C. Over the course of a year, the equator absorbs more solar energy than can be dissipated through infrared radiation. Excess energy is transported toward the poles by winds (4/5 of the excess energy) and ocean currents (1/5). Since the poles and equator begin at the same temperature, excess heat has nowhere to go. As a result, the equatorial temperatures increase. As seen in Fig. 1a, ten years into the simulation equatorial waters reach 26 °C while the sea surface in the Arctic cools to 9 °C. Forty years into the simulation (Fig. 1b) the surface of the Arctic Ocean reaches freezing and

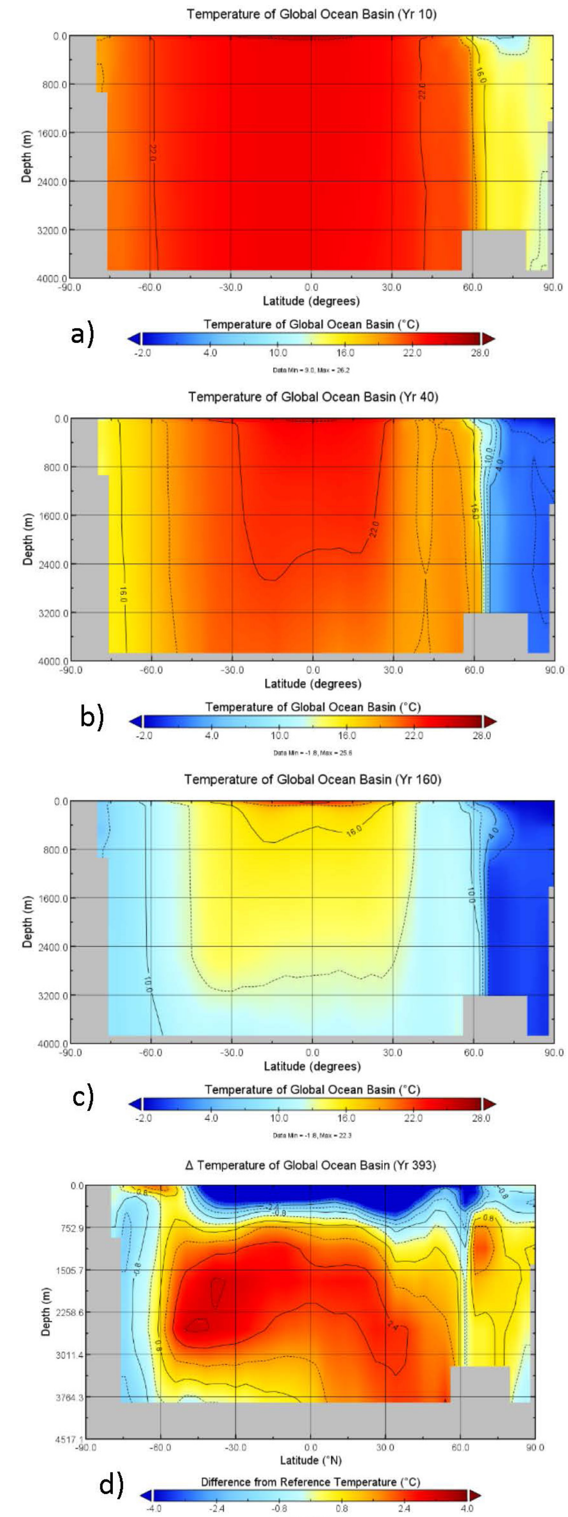

Figure 1. Ocean temperature plotted by latitude (South Pole to North Pole) and depth. Ocean temperature at a) 10 years, b) 40 years, and c) 160 years. d) Difference between ocean temperature at 393 years and modern-day values.

sea ice begins to form. By year 160 (Fig. 1c) the depth of the Arctic Ocean approaches the freezing point. The Arctic appears cut off from the circulation taking place in other oceans, which are becoming stratified with warm water pooling at the surface.

Fig. 1d is the difference between the model at the end of the simulation and modern-day ocean temperatures. The Arctic Ocean is close to modern day values with the deeper waters being slightly warmer. However, in the tropics and midlatitudes the surface waters are significantly cooler. This is due to the thick layer of stratospheric aerosols defined at the beginning of the simulation. Initially they help limit the amount of excess heating in the tropics. However, once the ocean cools it drives the earth system to a temperature that is cooler than current day values. It is anticipated that an extended run will eventually freeze the ocean surface at the equator leading to what is often called snowball earth.

Although the earth system is driven to colder values, a four hundred year simulation is not sufficient to cool the deep oceans to current day values. Sequestration of water in the form of ice sheets lowers sea level, but only several meters below current day values. If our scenario is to match conditions during the last ice age maximum, sea levels need to be 130 meters lower than they are today. Some of that comes from further cooling of the deep ocean. However, most is due to sequestration of water on the continents in the form of ice sheets. This hints at one deficiency of the model, which we will address later when we discuss the buildup of land ice.

Regarding ocean cooling, Marshall and Plumb (2008) indicate that a fully mixed ocean has a thermal adjustment time constant of 40 years. Beginning with 24 °C oceans, five time constants, or 200 years, should be sufficient to bring the oceans to a temperature within one percent of modern day values. As illustrated in Fig. 2, the average ocean temperatures cool exponentially. However, the time constant is 238 years. In addition, it is clear from Fig. 2 that the exponential model underestimates cooling during the later 150 years of the simulation. This is due to the thick layer of stratospheric aerosols overcooling the earth system. The buildup of land and sea ice in the higher latitudes also changes the earth's albedo, thus reducing the equilibrium temperature of earth.

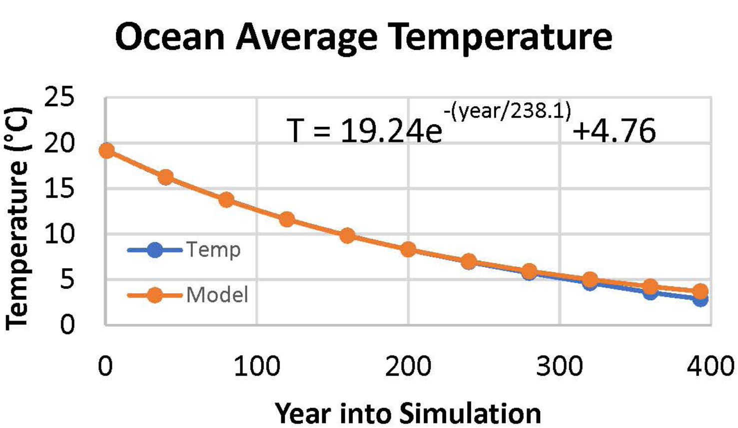

Figure 2. Average ocean temperature by year of simulation. The ocean cools exponentially towards an equilibrium temperature of 4.76. The actual temperature diverges towards the end of the simulation due to over cooling from stratospheric aerosols and buildup of ice sheets.

B. Ocean mixed layer depth

Under modern day conditions, the ocean surface is decoupled from the depths. Heating by the sun and atmosphere forms a stable layer of water near the ocean surface. Vertical circulation is restricted to the mixed layer. As seen in Fig. 3a, the mixed layer of the reference model is mostly restricted to the top fifty meters of the ocean. Deeper ocean mixing occurs between Greenland and England and off the coast of Antarctica. This is where cold surface waters sink to the ocean bottom and become part of the thermohaline circulation.

Ten years into the simulation (Fig. 3b) most of the ocean is experiencing circulation with cooler surface water driven to the bottom of the ocean. The only place where the mixed layer is shallow is near the equator where warm surface water forms a stable layer. By year

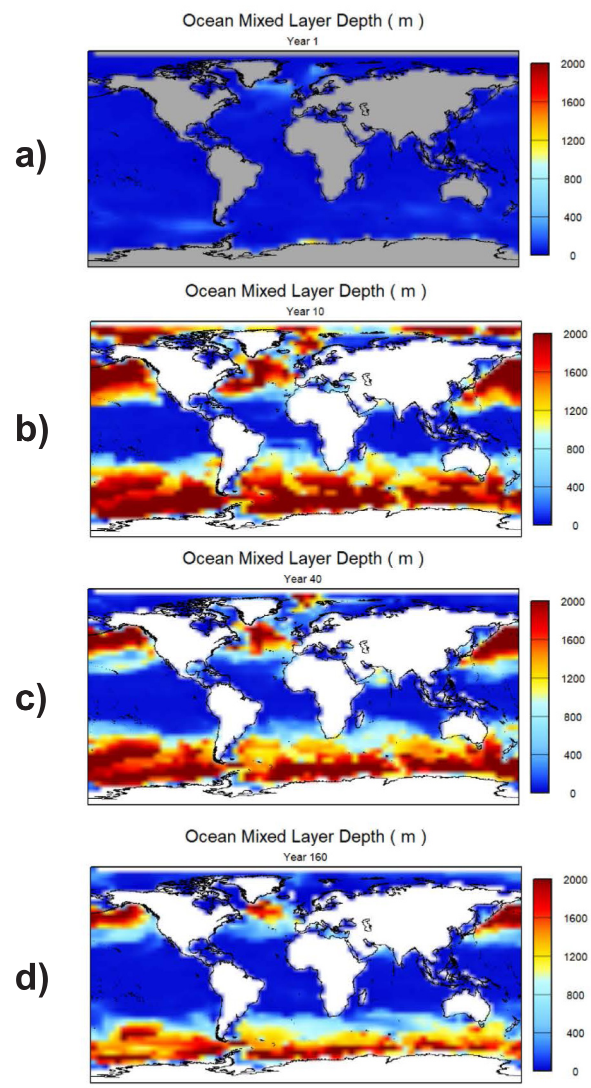

Figure 3. Ocean mixed layer depth. The reference model (a) indicates that most of the ocean has a mixed layer restricted to the surface. In the warm ocean model, b) deep convection occurs over most of the ocean in the first ten years of the simulation. c) By year forty convection in the Arctic is cut off and for the remainder of the simulation d) deep convection is restricted to the boundaries of open sea next to sea ice.

forty (Fig. 3c) most of the deep convection in the Arctic has disappeared. This is due to the formation of sea ice in the Arctic. In year 160 (Fig. 3d) deep mixing occurs at the edge of the sea ice in the Arctic and off the coast of Antarctica. This pattern continues to the end of the simulation. If the simulation were extended, it is anticipated that the deep ocean will cool further resulting in a decoupling of deep ocean and surface circulations. This results in slower deep ocean circulation, which may affect proxy indicators, such as sea floor sediments.

C. Sea surface temperature and sea ice thickness

Having looked at the vertical circulation within the ocean, it is important to look at its effect on the surface. Fig. 4a plots the sea surface temperature ten years into the simulation. Although the Arctic Ocean has cooled, the surface is still around 14 °C. At the equator, surface temperatures have risen to 26 °C. By year forty (Fig. 4b) Arctic waters are below freezing allowing the formation of sea ice. Equatorial waters can now circulate excess heat to the poles and begin to cool. Fig. 4c corresponds to year 160 of the simulation. Surface waters at the freezing point form an arc that extends from Nova Scotia along the coast of Greenland to Great Britain. By the end of the simulation (Fig. 4d), that arc extends further south to form a line between Maine and France.

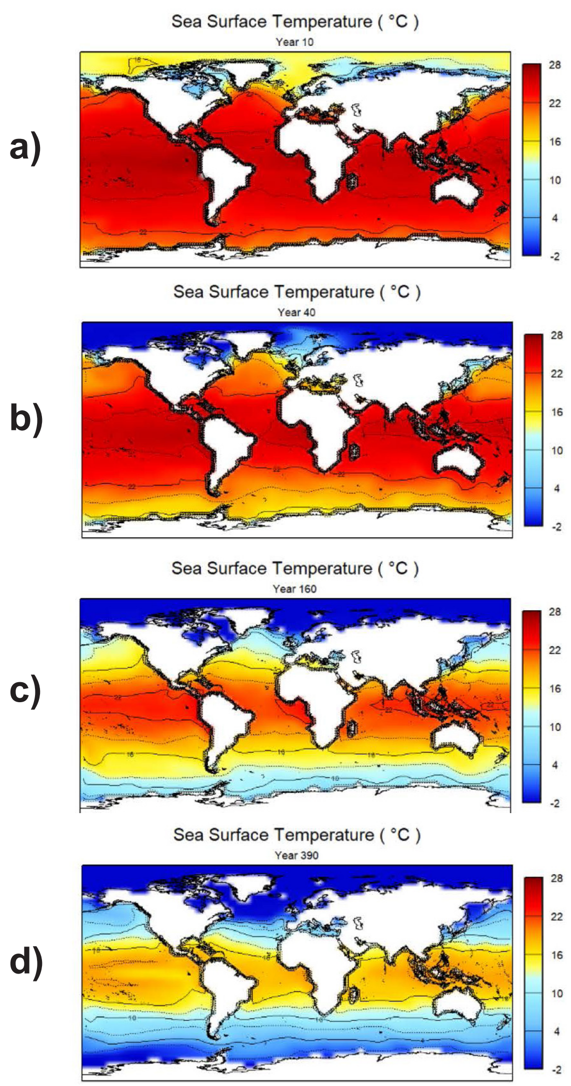

Figure 4. Sea surface Temperature for various years in the simulation. a) Ten years, b) forty years, c) 160 years, and d) 390 years.

In the Pacific unfrozen ocean extends to the coast of Alaska. Given the shallow connecting basin between the Pacific and Arctic Oceans, circulation begins to restrict by year forty (Fig. 5a). At year 160 (Fig. 5b) sea ice in the Arctic has thickened considerable. This trend continues until the Pacific is cut off from the Arctic. In the Atlantic some circulation with the Arctic continues through the ocean near Iceland. However, most of the Atlantic's vertical circulation occurs at the boundary between sea ice and open ocean.

Looking closely at Fig. 5b, we see a gray region off the coast of Greenland towards Canada. This represents sea ice thickness greater than sixty meters. During the simulation the model stopped several times due to a low ocean mass error. Upon consultation with the model user group, it was revealed that some dynamics of the ocean are not calculated for layers near the surface. As sea ice thickens, it impinges on deeper layers resulting in an error. Initial errors were recoverable; however, by year 165 the model failed. Increasing the depth to layer three, corresponding to 57 meters, extended the life of the model to year 2270. An additional change of depth to layer four, 98 meters, allowed the model to reach year 393. Given the proximity to 400 years, the simulation was ended. By the end of the simulation, the sea ice abnormality off the coast of Greenland had reached the ocean floor, although most of the Arctic Ocean ice was only sixty meters thick. Increasing the depth to layers three and four influences ocean circulation and needs to be addressed in future research. One solution is to remove the sea ice anomaly by Greenland and see if the model will continue running using a minimum depth corresponding to layer two, 30 meters.

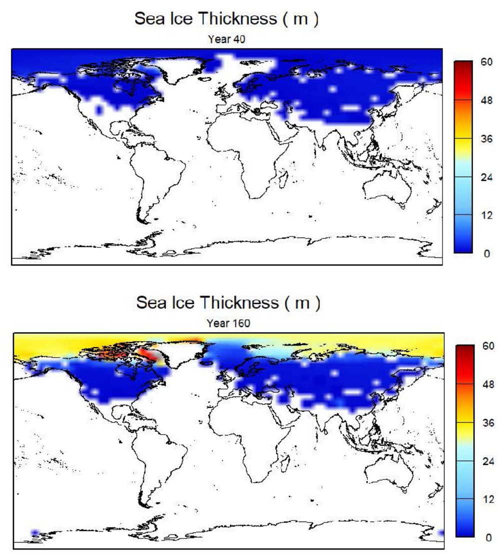

Figure 5. Sea ice thickness. a) Forty years into the model and b) 160 years. Since the model's sea ice field includes lake ice, there is ice present over the northern continents.

D. Surface air temperature

Surface air temperatures follow an expected pattern. During year one

(Fig. 6), before the ocean has a chance to cool, air temperatures are warm from pole to pole. These above zero temperatures persist over the Arctic through year ten, preventing ice accumulation over the ocean. During the winter season land masses located at higher latitudes cool below the freezing point allowing snowfall. The same is true for Antarctica during the Northern Hemisphere summer. Equatorial air temperatures exceed 30 °C, but decline as the oceans cools. Fig. 7 shows the seasonal temperatures for year forty. By this time,

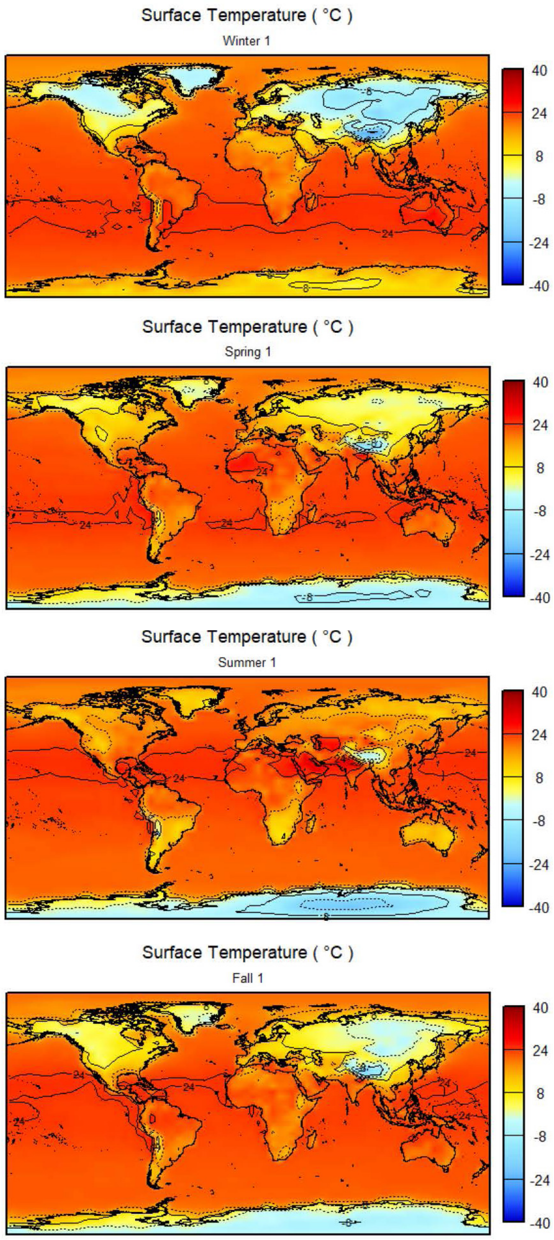

Figure 6. Average high surface air temperature for the four seasons during year one.

air over the Arctic Ocean remains below freezing year-round. This is important for the accumulation of snow and sea ice.

By the time the simulation reaches year 160 (Fig. 8), Arctic temperatures extend below –40 °C, as indicated by the gray regions. During

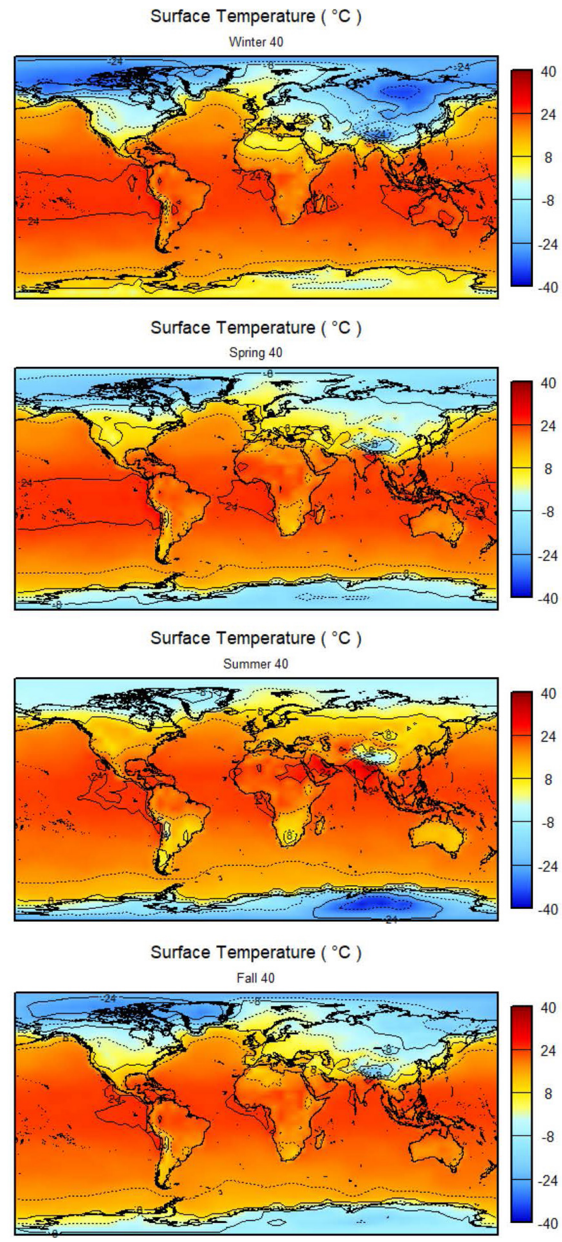

Figure 7. Average high surface air temperature for the four seasons during year forty.

the winter, average freezing temperatures extend to the Gulf of Mexico. During the summer, temperatures rebound to 14 °C; however, this is well below current temperatures. By the time the model reaches year 390 (Fig. 9), temperatures over the Midwestern United States reach an average temperature high of 6 °C. The equatorial highs at the end of the model are only in the low twenties. This is another indicator that the stratospheric aerosols are having an undue impact by the end of the simulation.

E. Precipitation

As pointed out in Spelman (1996) and Gollmer (2013), a warm Arctic Ocean results in significant precipitation during a perpetual January simulation. Fig. 10 confirms this and indicates strong precipitation during the spring and fall. However, this precipitation is

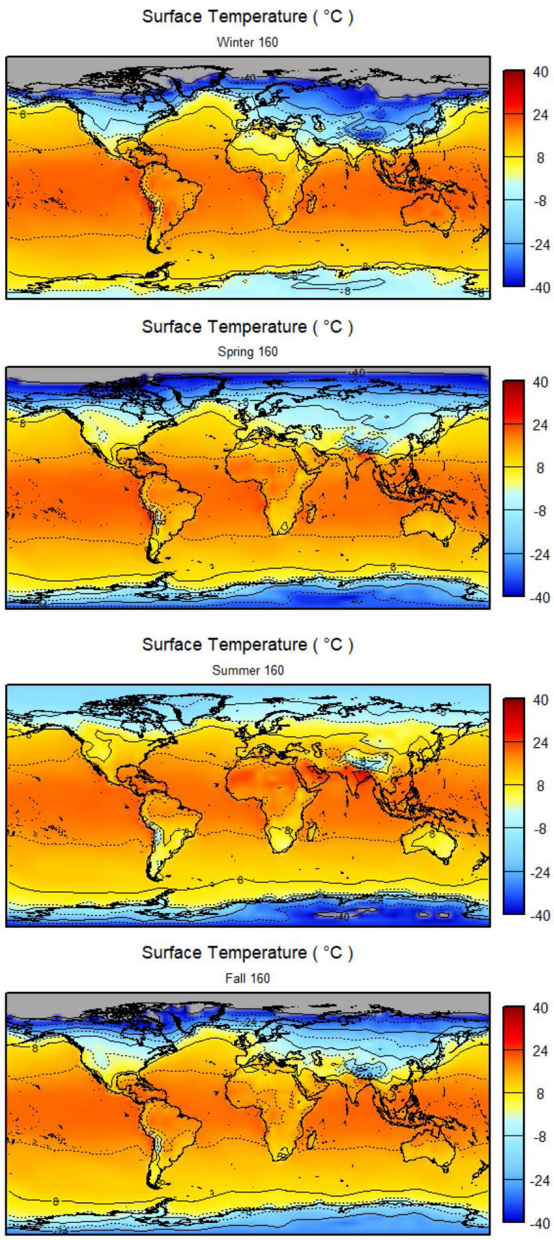

Figure 8. Average high surface air temperature for the four seasons during year 160.

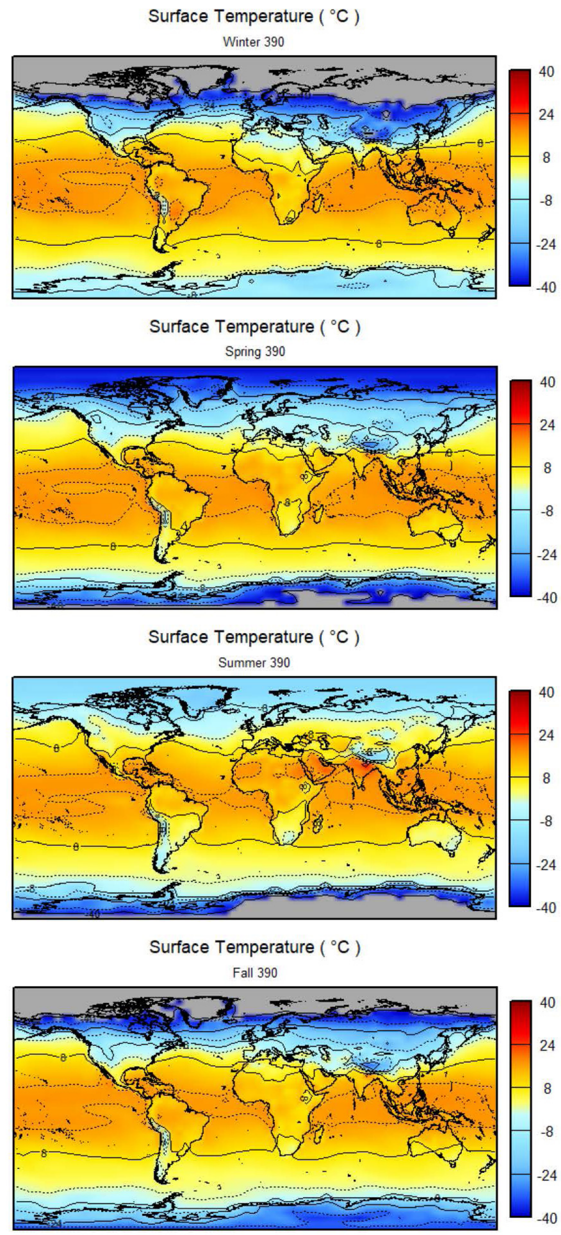

Figure 9. Average high surface air temperature for the four seasons during year 390.

in the form of rain due to the warm air and sea surface temperatures. This precipitation is also primarily over the ocean. By year ten (Fig. 11), precipitation in the Arctic has subsided. A pocket of intense precipitation persists next to Alaska and Northern Canada due to moist ocean air driven over cold land masses by the jet stream. However, this effect does not generate large amounts of precipitation over Eastern Canada and the Great Lakes region. There is precipitation over the Atlantic next to Greenland's coast, but it does not penetrate inland, which would aid in building up an ice sheet.

Fig. 12 shows the seasonal precipitation pattern for year forty. Precipitation along the western coast of North America continues to be strong and increasingly so along the coast of Greenland during the winter. By this time in the simulation, precipitation has dropped off over most of the Arctic. Sea ice covers the ocean surface, cutting off a major source of water vapor. The reduction in precipitation over the Arctic is clearly seen by year 160 (Fig. 13). Sea ice is thirty meters thick and water vapor comes from evaporation off the ice rather than open water.

F. Snowfall and snow depth

Combining what is observed about ocean/air temperature and precipitation patterns, it is possible to explain the snowfall pattern. Early in the simulation, snowfall is insignificant due to the warm ocean and air temperatures. However, by year ten (Fig. 14) temperatures have fallen enough for snowfall to occur over land during the hemisphere's winter season. Snowfall up to 2 mm/day is present in Canada, Scandinavia, Asia, and Antarctica. Over the winter season this results in an accumulation of 0.2 meters. However, during the summer season,

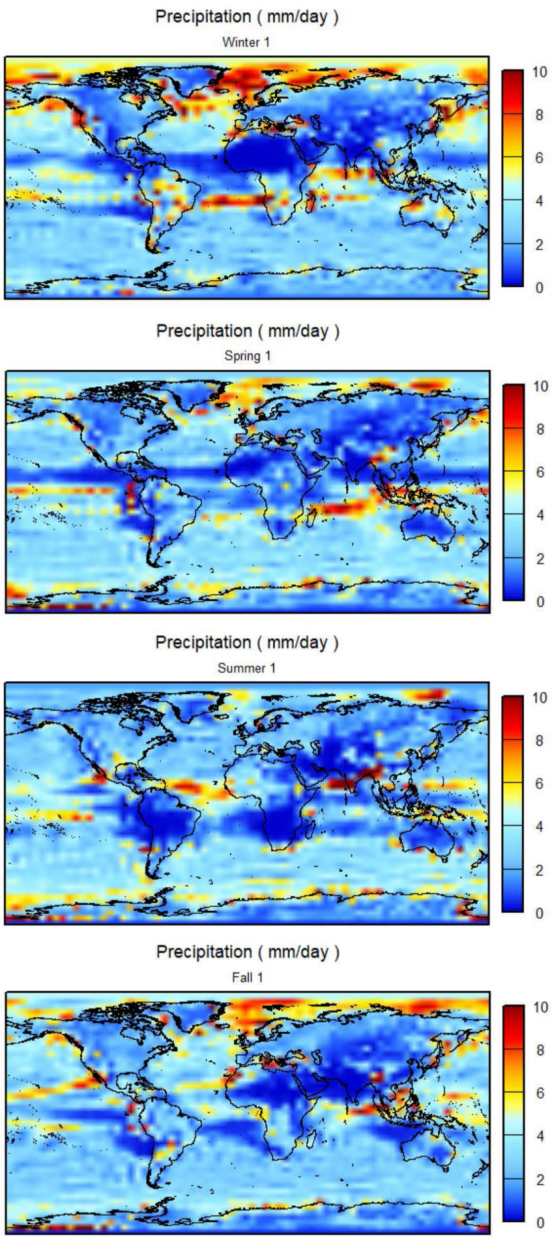

Figure 10. Precipitation for the four seasons during year 1.

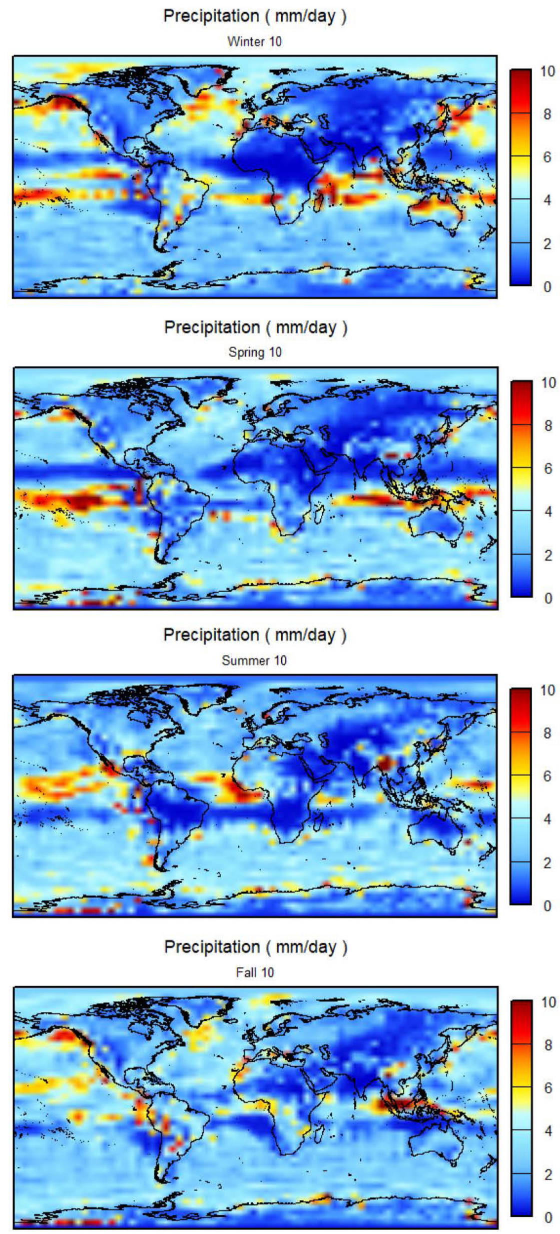

Figure 11. Precipitation for the four seasons during year 10.

this melts away. Year forty (Fig. 15) has snowfall occurring during all four seasons in the Arctic and Antarctic. This is a result of sea ice covering the Arctic Ocean, as seen in Fig. 5, and below freezing air temperatures (Fig. 7). Comparing snowfall and precipitation rates (Fig. 12), it appears snowfall is more intense. However, this is due to the color scale for snowfall maxing out at 3 mm/day. The pocket of high winter precipitation to the east of Greenland corresponds to the presence of open water. Sea ice extends towards the lower latitudes by year 160 and the snowfall pattern matches this advance (Fig. 16). By the end of the simulation (Fig. 17) snowfall occurs year-round as far south as the Mediterranean and to the southern tips of South America and Africa.

The simulation also tracks the accumulative effect of snowfall. No accumulation occurs during the first decade of the model. By year twenty, inland parts of Greenland can accumulate several meters of snow. Fig. 18 shows the state of the snowfield at year forty. Most of Greenland is covered with up to four meters of snow. At year 160 (Fig. 19) the depth of Greenland's snow is relatively unchanged. However, Antarctica has caught up with Greenland. By the end of the simulation, snow depth as illustrated in Fig. 19 has not changed appreciably in the subsequent 230 years.

Snow depth is only part of the picture. Fig. 20 shows the total earth ice at year forty. Since the scale is in kg/m^2, ice thickness in millimeters is approximated by dividing the given number by 0.90. Most of the ice accumulation is in Alaska and Northern Siberia. By year 160 (Fig. 21) the extent of significant ice cover has spread across Northern Europe and Canada. Fig. 22 corresponds to year 390 and has one meter of ice around the Great Lakes. Curiously, Greenland and Antarctica are not accumulating any significant ice, although the snow depth from Fig. 19 is greater than that over Canada. There does

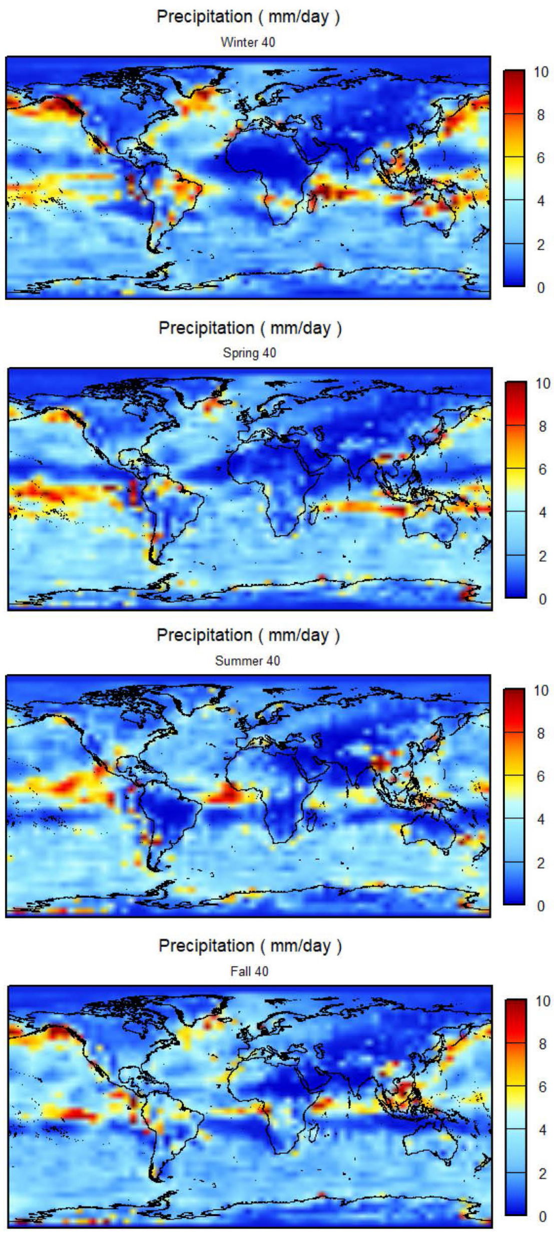

Figure 12. Precipitation for the four seasons during year 40.

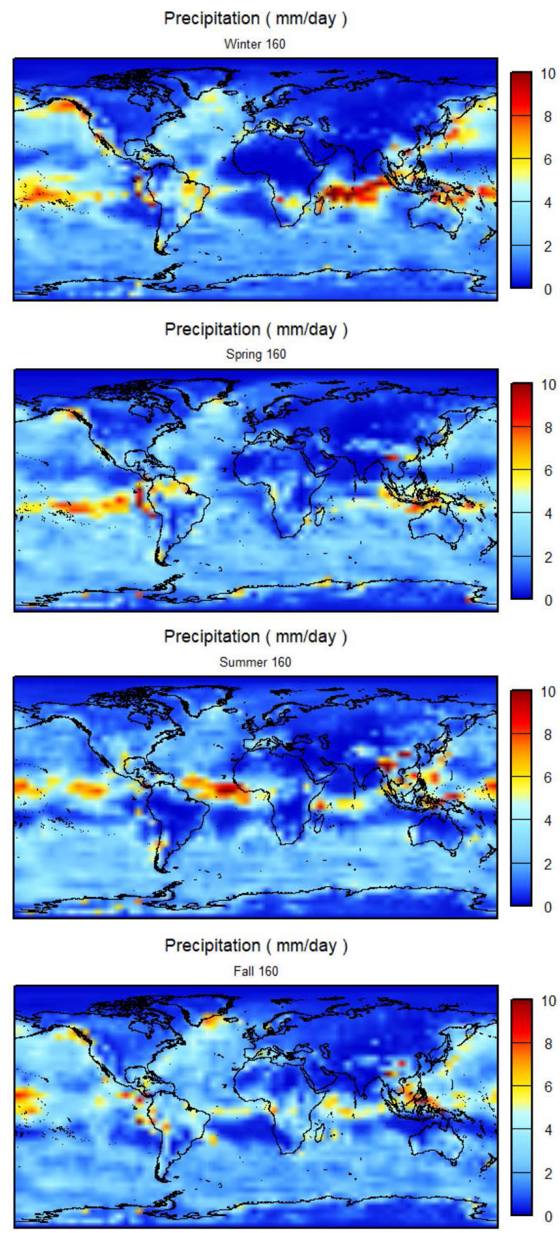

Figure 13. Precipitation for the four seasons during year 160.

not seem to be any data fields recording ice cover for these two regions. Since this simulation removes ice sheets over Greenland and Antarctica without changing the ground type, the model may be ignoring any ice accumulation in these regions. This also may explain why snow thickness is not increasing. It is converted to ice, but not recorded by the model. This is an anomaly that must be investigated in the future.

IV. DISCUSSION

A. Cooling oceans and precipitation

At the beginning of the simulation, warm oceans drive the climate. Although intense precipitation occurs over the open waters of the Arctic, within a decade it drops off as the surface of the ocean cools. This is disappointing since a major component of Oard's (1979) rapid ice age model depends on evaporation from the surface of the Arctic Ocean. Previous climate work supported Oard's conjecture; however, failed to capture the impact of the cooling ocean.

In addition, warm oceans prevent any accumulation of snow. The strength of this simulation is the use of a dynamic ocean. Once the sea surface cools sufficiently, snow begins to fall and sea ice forms. The fact that Greenland and Antarctica begin to accumulate snow and ice while the oceans are warmer than present day gives hope that future modeling may discover parameters that will generate the desired snowfall rate.

Although ocean cooling occurs slower than predicted by Marshall and Plumb (2008), ideal conditions for significant snowfall in North America are not long lived. Oceans initialized at 24 °C are cooled through convective circulation. This ignores any heat exchange between the ocean and ocean floor. If they were initially warmed by crustal motion, it is reasonable to assume they would continue to

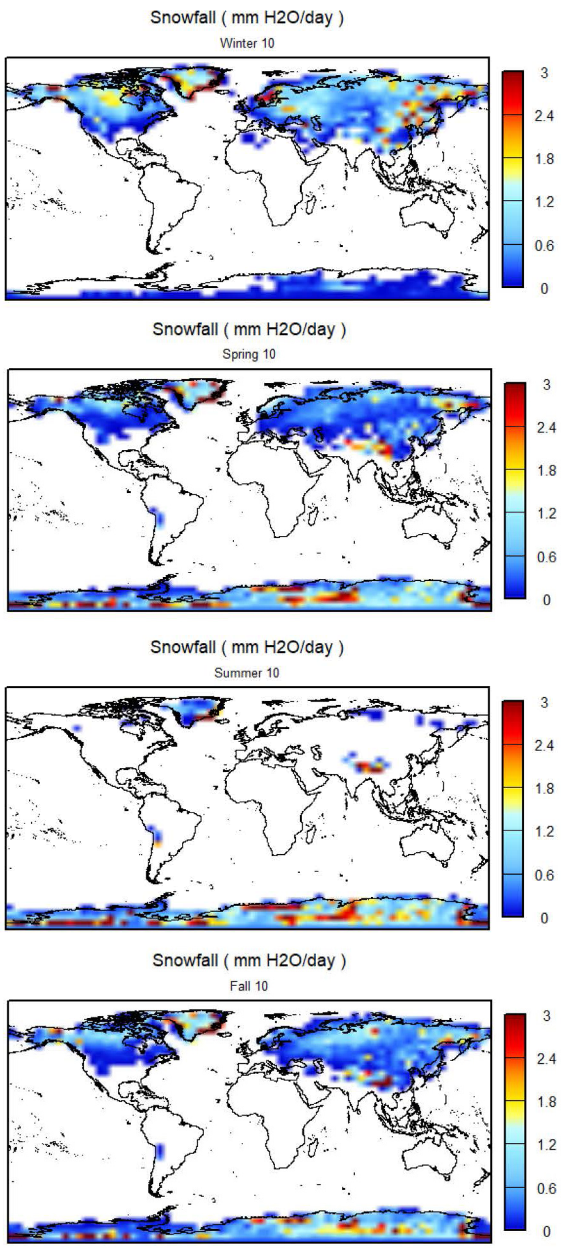

Figure 14. Snowfall for the four seasons during year 10.

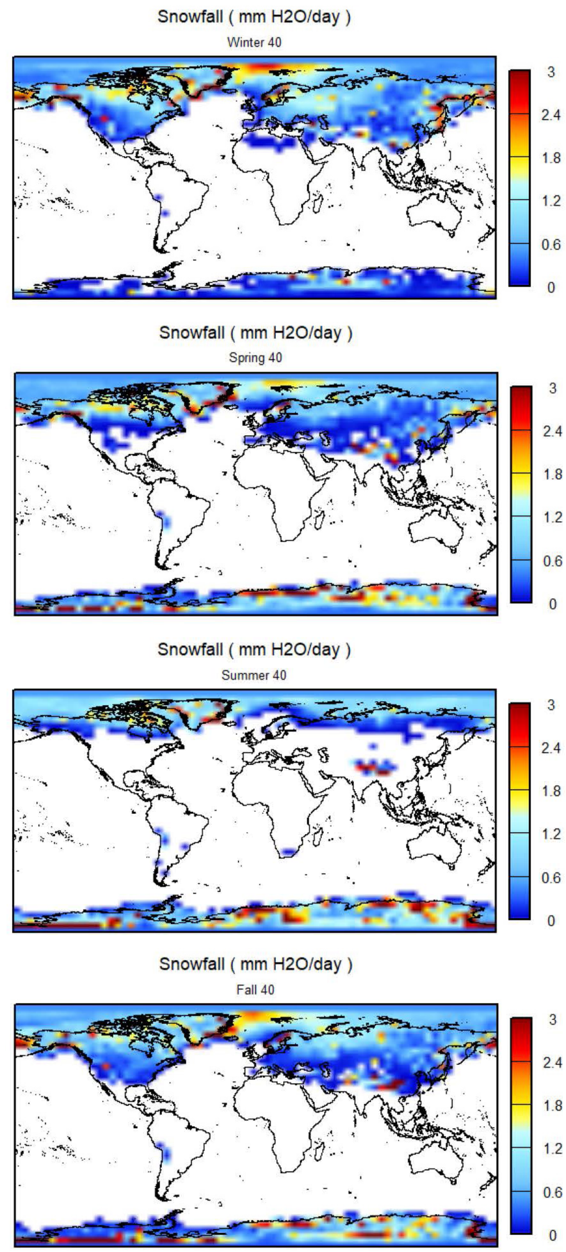

Figure 15. Snowfall for the four seasons during year 40.

absorb heat from the floor years into the simulation. It is not obvious how to incorporate this in the model without adding subroutines to the code. However if done, it would slow the transition between a warm ocean and an ice covered ocean.

It is the author's opinion that a low-resolution climate model may be insufficient to generate sufficient snowfall rates regardless of adjusting parameters. Snowfall rates are given in millimeters of equivalent liquid water per day. Across the Midwestern United States, the model predicts a half millimeter per day. Over a winter season, that comes to 45 mm of liquid water equivalent, or 46 cm of fluffy snow. A severe winter storm can deliver at least half of that amount over the course of several days. If the transitioning post-flood climate generates more frequent intense storms, it is reasonable to expect higher rates of snow accumulation.

Vardiman and Brewer (2012) pursued this line of reasoning using a mesoscale model. Instead of modeling grid cells 500 km on a side, the mesoscale model uses cells on the order of 30 km on a side. With a higher resolution, intense precipitation events within low pressure systems are more accurately modeled. This extended simulation provides atmospheric and oceanic conditions needed for the growth of an ice sheet. If a mesoscale model were initialized with conditions corresponding to year 160 of this research, it would be possible to study severe storms originating over the ocean that then advect over a preexisting ice sheet.

B. Stratospheric aerosols

Stratospheric aerosols were introduced in the model to offset the warm ocean's influence on the atmosphere. Without them, air temperature at the equator can approach 40 °C. However, by using an

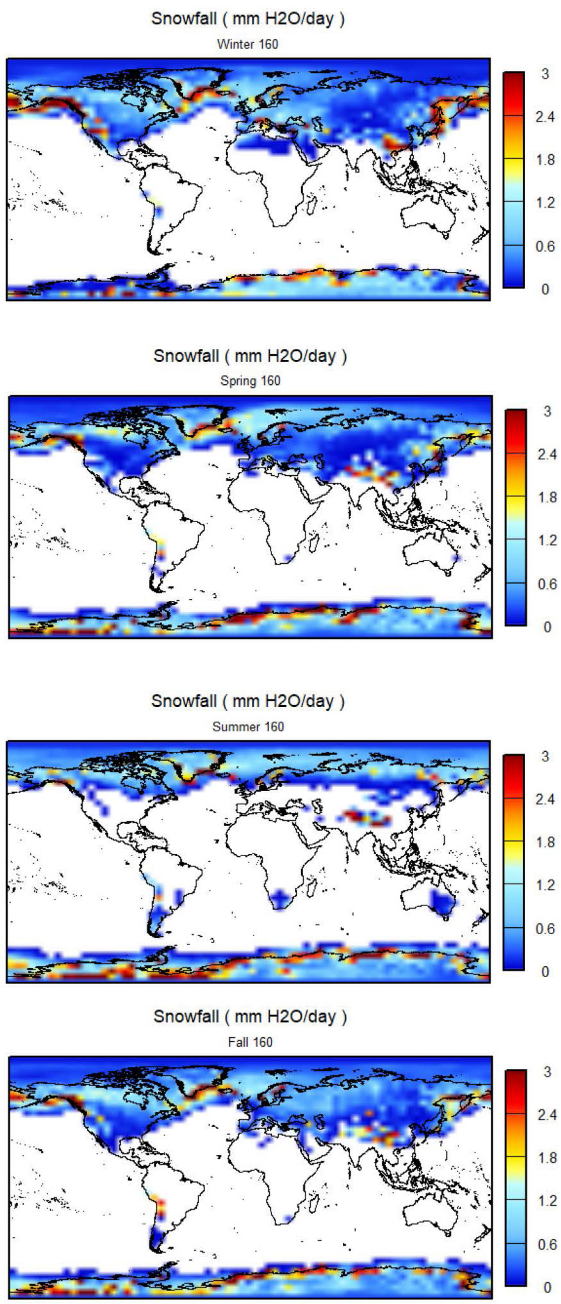

Figure 16. Snowfall for the four seasons during year 160.

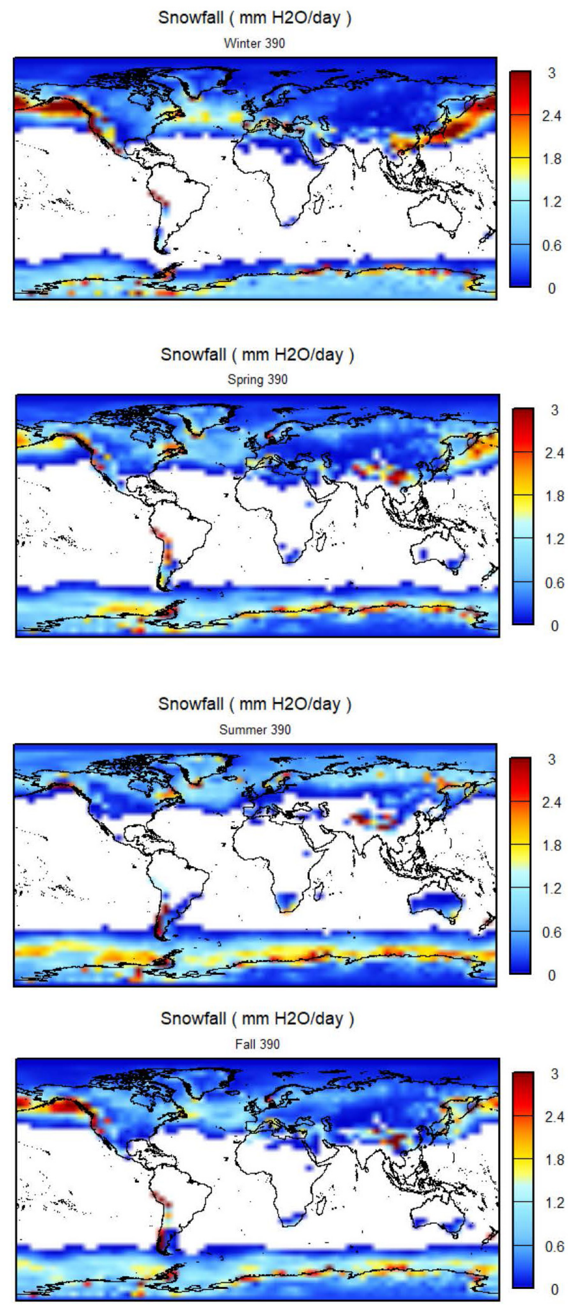

Figure 17. Snowfall for the four seasons during year 390.

optical thickness of 2.0 for the aerosols, the amount of direct sunlight reaching earth's surface is reduced to 13.5% of its original value. Although this works fine to keep temperatures in check early in the simulation, later it drives the surface air temperature below current day values. With the added reduction in absorbed sunlight due to increased reflectance by snow and ice, the earth is driven towards a final state where the surface is completely frozen.

Future modeling scenarios can take one of two approaches. The aerosol amount can be reduced as the simulation progresses. This is easily implemented since the model loads in a file, which specifies aerosol amount based on year. An alternate approach is initializing the simulation with cooler oceans and a commensurate lowering of aerosol amount. What those values are will require geological proxy

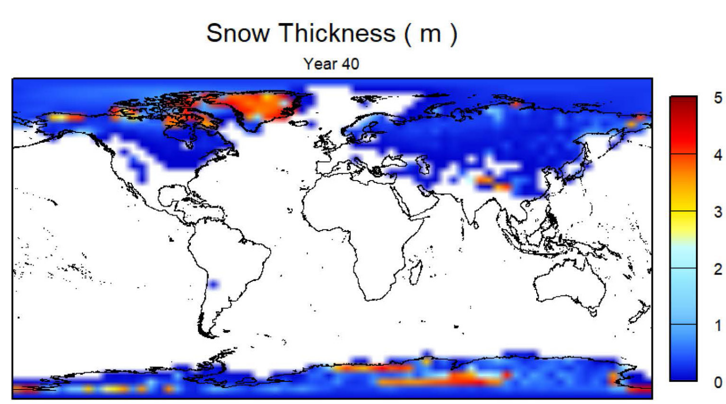

Figure 18. Snow thickness for year 40.

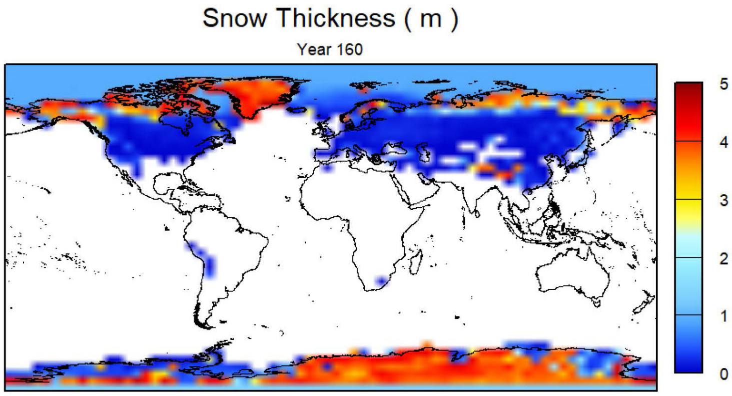

Figure 19. Snow thickness for year 160.

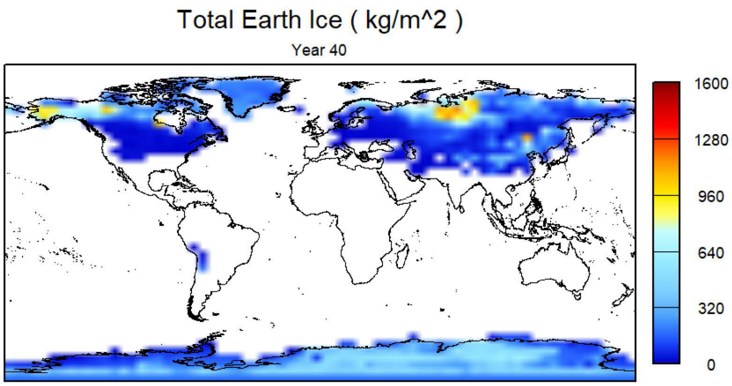

Figure 20. Total earth ice for year 40.

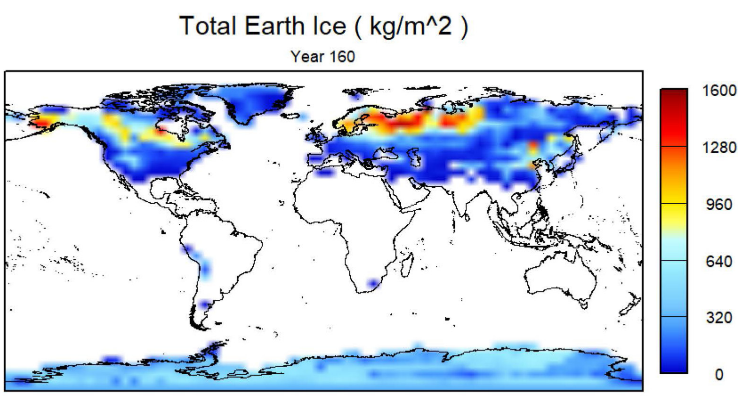

Figure 21. Total earth ice for year 160.

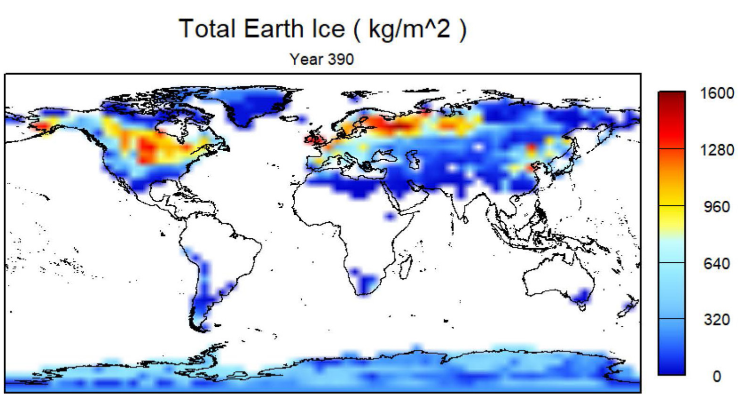

Figure 22. Total earth ice for year 390.

data to constrain the possibilities.

C. Model limitations

As mentioned previously, low resolution models fail to accurately capture sub-grid processes. However, there are other limitations to the model. According to Kelly et al. (2020), the GISS-E2.1 has a remnant double-ITCZ bias and is unable to provide a realistic stratospheric circulation. Although the current state of the model is greatly improved from previous models, there is consideration to move to an E3 model with higher resolution and new topologies.

The need to artificially move to deeper ocean minimums to avoid fatal run errors is also problematic. Although not a problem for simulations near current day conditions, it is for paleoclimate scenarios. The abnormal generation of thick sea ice off the coast of Greenland is an indication of tuned parameters pushed beyond their reasonable limits or an odd land/sea interaction that generated positive feedback.

Despite the limitations, this model is still useful for evaluating a rapid ice age scenario. Compared to other coupled climate models, implementation on a Linux system is well documented. Although run time speed is a factor, it does not require a supercomputer or specialized software to operate. The generated output is in NetCDF format, which is well supported by the scientific community.

V. CONCLUSIONS

This four-century simulation of a post-flood warm ocean world demonstrates that a climate model vetted by the scientific community can transition to a pre-ice age condition using a thick layer of stratospheric aerosols. Although precipitation and snowfall rates are not at the level required by Oard (1979), an ice-covered North America begins to take shape by the end of the simulation. Further research needs to identify specific ocean and surface conditions associated with enhanced snowfall and implement them in a higher resolution simulation of the GISS Model E2.1.2 or in a meso-scale model. The role of stratospheric aerosols and deep ocean heating also needs to be studied to provide a more accurate representation of the post-flood world.

ACKNOWLEDGMENTS

I would like to thank the NASA Goddard Institute for Space Studies for developing and refining the Model E2.1.2 source code. The user community for this model was invaluable when resolving compilation errors and fatal code errors. Fig. 1 was generated by the Panoply Data Viewer, developed by Dr. Robert Schmunk. The remaining figures apart from Fig. 2 were generated using the R programming language. Packages developed by the R user community made it possible to input, analyze, and visualize the data.

REFERENCES

Austin, S.A., J.R. Baumgardner, D.R. Humphreys, A.A. Snelling, L. Vardiman, and K.P. Wise. 1994. Catastrophic Plate Tectonics: A Global Flood Model of Earth History. In *Proceedings of the Third International Conference on Creationism*, ed. R.E. Walsh. Pittsburgh, Pennsylvania: Creation Science Fellowship.

Cox, D.E. 1979. Controversy about ice ages, *Creation Research Society Quarterly*, 16:21-28.

Gollmer, S.M. 2013. Initial conditions for a post-flood rapid ice age. In *Proceedings of the Seventh International Conference on Creationism,* ed.

M.F. Horstemeyer. Pittsburgh, Pennsylvania: Creation Science Fellowship.

Gollmer, S.M. 2018. Effect of aerosol distributions on precipitation patterns need for a rapid ice age. In *Proceedings of the Eighth International Conference on Creationism,* ed. J.H. Whitmore. Pittsburgh, Pennsylvania: Creation Science Fellowship.

Hansen, J. *et al.* 1983. Efficient three-dimensional global models for climate studies: Models I and II. *Monthly Weather Review* 111:609-662.

Hausfather, Z. 2019. CMIP6: the next generation of climate models explained. CarbonBrief. Retrieved December 15, 2022 from https://www.carbonbrief.org/cmip6-the-next-generation-of-climate-models-explained/

Kamworapan, S. and C. Surussavadee. 2019. Evaluation of CMIP5 Global Climate Models for Simulating Climatological Temperature and Precipitation for Southeast Asia. *Advances in Meteorology*. Retrieved December 15, 2022 from https://doi.org/10.1155/2019/1067365

Kelley, M., G.A. Schmidt, L.S. Nazarenko, S.E. Bauer, R. Ruedy, G.L. Russell, et al. 2020. GISS-E2.1 Configurations and Climatology. *Journal of Advances in Modeling Earth Systems*. Retrieved December 15, 2022 from https://doi.org/10.1029/2019MS002025

Luthi, D., *et al*. 2008. High-resolution carbon dioxide concentration record 650,000-800,000 years before present, *Nature*, 453:379-382.

Lyell, C. 1833. *Principles of geology: or, the modern changes of the earth and its inhabitants considered as illustrative of geology*. Salt Lake City: Project Gutenberg Literary Archive Foundation.

Marshall, J. & Plumb, R.A. (2008), Atmosphere, ocean, and climate dynamics: An introductory text, *Elsevier Academic Press*, Amsterdam.

Molen, M. 1990. Diamictites: ice-ages or gravity flows?, In *Proceedings of the Second International Conference on Creationism*, R.E. Walsh, *et al*, Editors, Pittsburgh, Pennsylvania: Creation Science Fellowship.

Oard, M.J. 1979. A rapid post-flood ice age, *Creation Research Society Quarterly*, 16:29-37.

Oard, M.J. 1990. *An ice age caused by the Genesis Flood*. Institute for Creation Research, El Cajon, CA.

Oard, M.J. 1997. A classic tillite reclassified as a submarine debris flow, *CEN Technical Journal*, 11:7.

PCMDI, 2007. CMIP3 Climate Model Documentation, References, and Links (Program for Climate Model Diagnosis & Intercomparison). Retrieved December 15, 2022 from https://pcmdi.llnl.gov/ipcc/model_documentation/ipcc_model_documentation.html

Schaeffer, F. 1972. *Genesis in space and time: the flow of biblical history*. Downers Grove, IL: InterVarsity Press.

Schmidt, G.A., *et al.* 2014. Configuration and assessment of the GISS ModelE2 contributions to the CMIP5 archive. *Journal of Advances in Modeling Earth Systems* 6:141-184.

Sluijs, A., *et al.* 2006. Subtropical Arctic Ocean temperatures during the Palaeocene/Eocene thermal maximum. *Nature* 441:610-613.

Spelman, K.E. 1996. A Sensitivity study of the post-flood climate using the NCAR CCM1 model with a warm sea-surface temperature, *ICR Thesis*, ICR Graduate School, El Cajon, CA.

Vardiman, L. 1998. Numerical simulation of precipitation induced by hot mid-ocean ridges, *Proceedings of the Fourth International Conference on Creationism*, R.E. Walsh, *et al*, Editors, Pittsburgh, Pennsylvania: Creation Science Fellowship.

Vardiman, L., A.A. Snelling, and E.F. Chaffin. eds. 2005. Radioisotopes and the age of the earth: Results of a young-earth creationist research initiative, vol. 2. El Cajon, California: Institute of Creation Research: Chino Valley, Arizona: Creation Research Society.

Vardiman, L. 2003. Hypercanes following the Genesis flood. In *Proceedings of the Fifth International Conference on Creationism*, ed. R.L. Ivey, pp. 17-28. Pittsburgh, Pennsylvania: Creation Science Fellowship.

Vardiman, L. and W. Brewer. 2010. Numerical simulation of precipitation in Yosemite National Park with a warm ocean: a pineapple express case study. *Answers Research Journal* 3:23-36.

Vardiman, L., and W. Brewer. 2011. A well-watered land: numerical simulations of a hypercyclone in the Middle East. *Answers Research Journal* 4:55-74.

Vardiman, L., and W. Brewer. 2012. Numerical simulation of three nor'easters with a warm Atlantic Ocean. *Answers Research Journal* 5:39-58.

Whitcomb, J.C. and H.M. Morris. 1961. *The Genesis flood: the biblical record and its scientific implications*. Grand Rapids, Michigan: Baker Book House.

Whitmore, J.H., and P.A. Garner. 2018. The Coconino Sandstone (Permian, Arizona, USA): Implications for the origin of ancient cross-bedded Sandstones. In *Proceedings of the Eighth International Conference on Creationism*, ed. J.H. Whitmore, pp. 581–627. Pittsburgh, Pennsylvania: Creation Science Fellowship.

THE AUTHOR

Steven M. Gollmer is a Senior Professor of Physics at Cedarville University. He holds a PhD in Atmospheric Science from Purdue University. His research interests include analysis of satellite imagery and climate modeling. He teaches an honors course comparing different worldviews as they relate to questions of physical, biological, and human origins.